



RESEARCH MEMORANDUM

PRELIMINARY ANALYSIS OF OVER-ALL PERFORMANCE OF AN
EIGHT-STAGE AXIAL-FLOW RESEARCH COMPRESSOR
WITH TWO LONG-CHORD TRANSONIC INLET STAGES

By Gilbert K. Sievers, Richard P. Geye, and James G. Lucas

Lewis Flight Propulsion Laboratory
Cleveland, Ohio

NATIONAL ADVISORY COMMITTEE
FOR AERONAUTICS

WASHINGTON
February 10, 1958
Declassified July 28, 1960

NATIONAL ADVISORY COMMITTEE FOR AERONAUTICS

RESEARCH MEMORANDUMPRELIMINARY ANALYSIS OF OVER-ALL PERFORMANCE OF AN EIGHT-STAGE
AXIAL-FLOW RESEARCH COMPRESSOR WITH TWO LONG-CHORD
TRANSONIC INLET STAGES

By Gilbert K. Sievers, Richard P. Geye, and James G. Lucas

SUMMARY

The chords of the first two stages of the eight-stage axial-flow compressor with two transonic inlet stages were doubled, and the over-all performance of the modified compressor was investigated over a range of weight flows at equivalent speeds from 30 to 100 percent of design at a constant high Reynolds number of approximately 2,250,000. At design speed, the maximum total-pressure ratio was 10.76 at an equivalent weight flow of 69.4 pounds per second with an adiabatic efficiency of 0.81, and the maximum equivalent weight flow was approximately 71.5 pounds per second ($30.1 \text{ (lb/sec)}/\text{sq ft}$ of frontal area). A peak efficiency of 0.69 was obtained at 50 percent of design speed, and a maximum peak efficiency of approximately 0.83 was obtained at 90-percent design speed. At the operating points investigated in a range from approximately 50 to 80 percent of equivalent design speed, the compressor had no periodic flow fluctuations such as are usually observed when rotating stall occurs.

The long-chord compressor had a larger stable operating range from 60 percent to design speed than the medium-chord compressor. The long-chord compressor attains higher efficiencies at the lower compressor speeds and approximately the same efficiency level at the higher compressor speeds. The stall margin for the fixed-exhaust-nozzle-area equilibrium operating line estimated for the long-chord compressor as a turbojet-engine component is roughly comparable to the stall margin for a 10-percent-increased exhaust-nozzle-area equilibrium operating line estimated for the medium-chord compressor.

INTRODUCTION

As part of the program to study the performance problems of multi-stage compressors with high-pressure-ratio, high Mach number stages, the eight-stage axial-flow compressor reported in references 1 to 7 was

modified by doubling the chord lengths of the first two stages, which were of transonic design. The aerodynamic design of this long-chord compressor is the same as that reported in reference 4.

The over-all performance characteristics of the compressor of this report were obtained over a range of weight flow for equivalent speeds from 30 to 100 percent of design speed and inlet pressures ranging from 20.3 to 10.1 inches of mercury absolute. The inlet pressure was varied in order to maintain a constant high Reynolds number of approximately 2,250,000 at all speeds except 30 percent of design speed. At 30 percent of design speed, a single point was obtained at a Reynolds number of approximately 1,270,000 instead of 2,250,000 because of inlet pressure limitations. The Reynolds number used in this report is based on relative conditions at the tip of the first rotor. Some of the results of reference 6 are compared with the results for the present compressor, and an estimated equilibrium operating line for a turbojet engine is superimposed on the compressor performance map to indicate the part-speed problems associated with the installation of this compressor in a turbojet engine.

SYMBOLS

- A frontal area, sq ft
c chord length at tip of first rotor, ft
P absolute total pressure, in. Hg abs
Re Reynolds number relative to first rotor tip, $\rho V' c / \mu$
T total temperature, $^{\circ}$ R
V' velocity relative to first-rotor tip, ft/sec
w weight flow, lb/sec
 δ ratio of inlet total pressure to NACA standard sea-level pressure of 29.92 in. Hg abs
 η adiabatic temperature-rise efficiency
 θ ratio of inlet total temperature to NACA standard sea-level temperature of 518.7° R
 μ viscosity based on total temperature at tip of first rotor, lb/(ft)(sec)
 ρ static density at tip of first rotor, lb/cu ft

Subscripts:

- 0 inlet depression-tank station
1 compressor-inlet measuring station
20 compressor-discharge measuring station

APPARATUS AND INSTRUMENTATION

Compressor

A cross-sectional view of the compressor, the inlet bellmouth nozzle, and the discharge collector is shown in figure 1. The aerodynamic design details for this compressor are the same as those presented in references 1 and 4, the one difference being the increased chord lengths of the first- and second-stage rotor and stator blades. The compressor of this report will be referred to as the long-chord compressor; the compressor of reference 6 will be referred to as the medium-chord compressor, because the blade chords of the first two stages are longer than typical blade chords in use in present-day compressors.

The first-stage rotor of this report is compared with the medium-chord rotor of reference 6 in figure 2. The chords of the first two stages were increased as follows:

First stage: Rotor tip from 3.766 to 7.517 in.
 Stator tip from 1.900 to 3.420 in.

Second stage: Rotor tip from 3.50 to 6.782 in.
 Stator tip from 1.950 to 3.671 in.

The medium-chord compressor had 20 and 23 blades, respectively, in the first- and second-stage rotors and 27 and 32 blades, respectively, in the first- and second-stage stators. The long-chord compressor had 10 and 12 blades, respectively, in the first- and second-stage rotors and 15 and 17 blades, respectively, in the first- and second-stage stators. Tip solidity and diameter were not changed. Because of an error in fabrication, the first-rotor blade-setting angles are higher than design at the hub, ranging from approximately 4.0° at the hub to 2.0° at the mean blade section. All other blade-setting angles and blade loading were unchanged.

The major compressor design values are:

Total-pressure ratio	10.26
Equivalent weight flow, lb/sec	72.4
Equivalent tip speed, ft/sec	1218
Relative tip Mach number	1.25
Inlet hub-tip diameter ratio	0.46
Diameter at inlet to first rotor, in.	20.86

Installation

The compressor was driven by a 15,000-horsepower variable-frequency electric motor. The speed was maintained constant by an electronic control and was measured by both an electric chronometric tachometer and an electronic frequency-period counter. Air entered the compressor through a submerged thin-plate orifice, a butterfly inlet throttle for controlling inlet pressure, and a depression tank 6 feet in diameter and approximately 10 feet long. Screens in the depression tank and a bellmouth faired into the compressor inlet were used to obtain a uniform distribution of air entering the compressor. Air was discharged from the compressor into a collector connected to the laboratory altitude exhaust system. Air weight flow was controlled by a butterfly valve located in the exhaust ducting.

Instrumentation

The axial locations of the instrument measuring stations are shown in figure 1. The inlet depression-tank station and the compressor-discharge station had axial locations that were in accordance with reference 8. The radial distribution of outlet total temperature was obtained from multiple-probe rakes located at the area centers of equal annular areas. The discharge static pressure was obtained from six wall static taps. The instruments used at each station are similar to those illustrated in reference 5. Temperatures were measured with self-balancing potentiometers, pressures with mercury manometers referenced to atmosphere for all compressor-inlet and -discharge pressures, and weight flow with a thin-plate submerged orifice.

PROCEDURE

The compressor was insulated with 4 inches of Fiberglas. An inlet temperature of approximately 400° R (-60° F) was maintained, and the Reynolds number relative to the tip of the first rotor was held constant at approximately 2,250,000 by controlling the inlet-air pressure. This Reynolds number was chosen in order to maintain approximately the same

inlet total temperatures and pressures at each compressor operating point that were used in the testing of the medium-chord compressor of reference 6.

The compressor was operated at 50, 60, 70, 80, 90, and 100 percent of equivalent design speed. At each speed a range of airflows was investigated from a maximum flow at which the compressor-discharge piping system was choked to a minimum flow at which compressor stall occurred. In addition, a single point was taken at 30 percent of equivalent design speed in order to determine the general location of the 30-percent operating line, and five points were taken at 75 percent of equivalent design speed in order to establish the location of the stall-limit line and the peak-efficiency point.

Radial surveys with a hot-wire anemometer were taken at various operating points to determine the presence of rotating stall. A single hot-wire-anemometer probe located behind the first-stage rotor and a dual-beam oscilloscope were used. Radial surveys were taken over the outer three-fourths of the passage at compressor speeds ranging from approximately 50 to 80 percent of equivalent design speed.

The over-all compressor performance characteristics were calculated from the orifice measurements, the drive-motor speed, the inlet total pressure and temperature, and the discharge static pressure and total temperature. The discharge total pressure was calculated by the procedure recommended in reference 8 and used in references 2, 3, 5, 6, and 7.

RESULTS AND DISCUSSION

Long-Chord-Compressor Performance

Over-all performance. - The over-all performance characteristics of the compressor with long-chord blades are presented in figure 3 as a plot of total-pressure ratio as a function of equivalent weight flow, with contours of constant adiabatic temperature-rise efficiency superimposed. The Reynolds number relative to the tip of the first rotor was maintained at approximately 2,250,000 for all compressor speeds except 30 percent of design speed. At design speed, a maximum total-pressure ratio of 10.76 (root-mean total-pressure ratio per stage of 1.346) was obtained at an equivalent weight flow of 69.4 pounds per second (29.2 (lb/sec)/sq ft of frontal area) with an efficiency of 0.81. A design-speed peak efficiency of 0.82 was obtained at total-pressure ratios ranging from 9.0 to 10.2, and a design-speed maximum weight flow of approximately 71.5 pounds per second (30.1 (lb/sec)/sq ft of frontal area) was obtained at pressure ratios below approximately 7.5.

There is a slight knee in the stall-limit line at approximately 62 percent of design speed. The stall-limit line can be approximated by two straight lines, one extending from 50 to 62 percent of design speed and the other from 62 percent to design speed.

The over-all adiabatic temperature-rise efficiency is plotted as a function of equivalent weight flow in figure 4. The peak efficiency at 50 percent of design speed is approximately 0.69. The peak efficiency increases slowly with speed and reaches a maximum value of approximately 0.83 at 90-percent design speed and then drops slightly at design speed.

Rotating stall. - No periodic flow fluctuations associated with rotating stall were observed at any of the operating points investigated in a range from approximately 50 to 80 percent of equivalent design speed. Random frequencies were observed at all radial probe positions and compressor speeds (partially because of blade wakes), but no periodic stall frequency could be detected. This is discussed further in a later section.

Comparison of Long-Chord and Medium-Chord Compressors

Over-all performance. - Figure 5 is a plot of total-pressure ratio as a function of equivalent weight flow for both the long-chord compressor of this report and the medium-chord compressor of reference 6. From 50 to 62 percent of design speed, the stall-limit lines are approximately the same. From approximately 62 percent to design speed, the long-chord compressor has an increased stable operating range. The medium-chord compressor has a slight knee in the stall-limit line at approximately 74 percent of design speed, whereas the knee in the long-chord compressor stall-limit line occurs at approximately 62 percent of design speed. From 50 to 70 percent of design speed, the long-chord compressor attained slightly higher equivalent weight flows and total-pressure ratios. At 75 percent of design speed, where the greatest improvement in stable operating range is found, the long-chord compressor attained a total-pressure ratio of approximately 4.7 at an equivalent weight flow of approximately 38.5 pounds per second as compared with 4.3 and 41.5, respectively, for the medium-chord compressor. From 80 percent to design speed, the long-chord compressor was able to operate at lower equivalent weight flows and attain approximately the same total-pressure ratios as the medium-chord compressor.

Adiabatic temperature-rise efficiency is plotted as a function of equivalent weight flow for both compressors in figure 6. In making this comparison, it must be remembered that the medium-chord compressor was uninsulated, while the long-chord compressor was insulated with 4 inches of Fiberglas to minimize heat-transfer losses through the casing. Therefore, the medium- and long-chord curves of figure 6 are not directly comparable because of different heat-transfer effects. However, a limited

amount of data was obtained at design speed with the medium-chord compressor insulated with 4 inches of Fiberglas. The results indicated that the efficiency at design speed was approximately the same as that of the long-chord compressor. It is reasonable to assume that heat transfer will affect the efficiency to a lesser degree at low compressor speeds than it will at higher compressor speeds because of the smaller over-all temperature rise. Therefore, a more representative comparison of efficiency levels could possibly be made if the higher-speed medium-chord curves were lowered slightly. Using these assumptions, the long-chord compressor attains higher efficiencies at the lower compressor speeds and approximately the same efficiency level at the higher compressor speeds. These increased efficiencies at part speeds are consistent with the more stable operating conditions (i.e., no rotating stall).

Rotating stall and operating range. - The medium-chord compressor of reference 6 had a rotating-stall region extending to approximately 74 percent of design speed. The long-chord compressor of this report had no periodic flow fluctuations, such as are usually observed when rotating stall occurs, at any of the operating points investigated in a range from approximately 50 to 80 percent of equivalent design speed. No quantitative explanation of this result can be given at the present time. However, it is believed that the explanation lies in the low number of blades and the resulting large spacing. The first-stage rotor consists of only ten blades with a spacing of approximately 6.54 inches at the tip. The unorthodox physical geometry of this design can best be appreciated by referring to figure 2(a).

Reference 9 states that there exists a lower limit to the number of blades that can support stall propagation. The geometry of this rotor is such that it probably falls below this lower limit. Reference 10 presents a theory by which some properties of rotating stall are predictable as long as the number of blades is high enough to justify the assumption of an infinite number of blades, and further states that the theory is unable to predict the influence of blade solidity on stall propagation when the blades are not close enough together. This discussion points out that theories of rotating stall in multistage turbomachinery are not very far advanced at the present time and are certainly not adequate to cover the findings of this investigation.

The doubling of the chords of the first two stages primarily affects the compressor performance in the intermediate-speed range. The extension of the stable operating range at part-speed could be logically expected if the inlet stages were able to operate over a larger flow range. Reference 11, which gives the results of investigating long- and short-chord single-stage-compressor rotors having the same solidity but different aspect ratios, shows that the long-chord or low-aspect-ratio rotor was able to operate over a wider flow range, attaining both higher and lower equivalent weight flows and higher total-pressure ratios than the short-chord

rotor. Therefore, either an increased chord length or a decreased aspect ratio does give an increased operating range. The geometry of the rotors of reference 11 is as follows:

	Rotor	
	Short-chord	Long-chord
Number of blades	66	26
Chord, in.	0.67	1.67
Passage height, in.	1.4	1.4
Tip solidity	≈ 1.0	≈ 1.0
Aspect ratio	2.09	0.84

Although the long-chord rotor had a larger stall-free range of operation, a rotating-stall region was encountered that was similar to that of the short-chord rotor. Consequently, these results are of no value in explaining the absence of rotating stall in the long-chord compressor of this report. However, the single-stage rotors did not approach the actual physical extremes of low blade number and large spacing encountered in the investigation reported herein.

Equilibrium operating lines. - Figure 7 is a comparison of the long-chord and medium-chord compressor maps with estimated equilibrium operating lines superimposed. The equilibrium operating lines were obtained by the approximate method of reference 12. In using this method, the following engine operating conditions at design speed were selected for sea-level static conditions: compressor pressure ratio, 9.0; ratio of turbine-inlet to compressor-inlet temperature, 4.0; and turbine efficiency, 0.85. The fuel-air ratios, 0.01572 for the long-chord and 0.01562 for the medium-chord compressor, were calculated according to the method of reference 13. At compressor pressure ratios less than 9.0, the turbine operating line used was for a multistage turbine (see ref. 12) with a constant efficiency of 0.85. With a fixed exhaust-nozzle area, the medium-chord operating line intersected the stall-limit line at approximately 76 percent of equivalent design speed (60 percent of maximum equivalent weight flow at a pressure ratio of 4.6), while the long-chord operating line lay entirely within the stable operating region, becoming tangent to the stall-limit line at approximately 60 percent of design speed (34 percent of maximum equivalent weight flow at a pressure ratio of 2.5). For the medium-chord operating line to lie entirely within the stable operating region, it was necessary to increase the exhaust-nozzle area by 10 percent, so that it became tangent to the stall-limit line at approximately 74 percent of equivalent design speed (55 percent of

maximum equivalent weight flow at a pressure ratio of 4.0). Actually, neither the long-chord operating line nor the increased-exhaust-nozzle-area operating line for the medium-chord compressor allows any margin for acceleration through the intermediate-speed range. Therefore, a larger exhaust-nozzle area would be necessary, or some other method such as bleed would have to be used to obtain acceleration margin for both compressors. The amount of exhaust-nozzle-area variation or bleed required for acceleration through the intermediate-speed range would be less for the long-chord compressor.

Another possible advantage of the long-chord compressor over the medium-chord as an engine component is the absence of rotating stall over the entire range of operation. This greatly lessens the likelihood of blade failure due to resonant vibration caused by unsteady aerodynamic loading.

SUMMARY OF RESULTS

The following results were obtained from an investigation of overall performance of an eight-stage axial-flow compressor with two long-chord transonic inlet stages:

1. The maximum total-pressure ratio obtained at design speed was 10.76 at an equivalent weight flow of 69.4 pounds per second with an adiabatic efficiency of 0.81.
2. A peak efficiency of 0.82 was obtained for design speed at values of total-pressure ratio ranging from 9.0 to 10.2.
3. A maximum equivalent weight flow of approximately 71.5 pounds per second ($30.1 \text{ (lb/sec)}/\text{sq ft}$ of frontal area) was obtained at design speed.
4. A peak efficiency of 0.69 was obtained at 50 percent of design speed; a maximum peak efficiency of approximately 0.83 was obtained at 90 percent of design speed.
5. Over a range of speeds from approximately 50 to 80 percent of equivalent design speed, the compressor had no periodic flow fluctuations such as are usually observed when rotating stall occurs.
6. The long-chord compressor has an increased stable operating range from 60-percent to design speed over that of the medium-chord compressor. The greatest improvement in operating range was obtained at 75 and 80 percent of equivalent design speed.

7. The long-chord compressor attains higher efficiencies than the medium-chord compressor at the lower compressor speeds and approximately the same efficiency level at the higher compressor speeds.

8. The stall margin for the fixed-exhaust-nozzle-area equilibrium operating line estimated for the long-chord compressor as a turbojet-engine component is roughly comparable to the stall margin for a 10-percent-increased exhaust-nozzle-area equilibrium operating line estimated for the medium-chord compressor.

Lewis Flight Propulsion Laboratory
National Advisory Committee for Aeronautics
Cleveland, Ohio, August 29, 1957

REFERENCES

1. Voit, Charles H.: Investigation of a High-Pressure-Ratio Eight-Stage Axial-Flow Research Compressor with Two Transonic Inlet Stages. I - Aerodynamic Design. NACA RM E53I24, 1953.
2. Geye, Richard P., Budinger, Ray E., and Voit, Charles H.: Investigation of a High-Pressure-Ratio Eight-Stage Axial-Flow Research Compressor with Two Transonic Inlet Stages. II - Preliminary Analysis of Over-All Performance. NACA RM E53J06, 1953.
3. Voit, Charles H., and Geye, Richard P.: Investigation of a High-Pressure-Ratio Eight-Stage Axial-Flow Research Compressor with Two Transonic Inlet Stages. III - Individual Stage Performance Characteristics. NACA RM E54H17, 1954.
4. Geye, Richard P., and Voit, Charles H.: Investigation of a High-Pressure-Ratio Eight-Stage Axial-Flow Research Compressor with Two Transonic Inlet Stages. IV - Modification of Aerodynamic Design and Prediction of Performance. NACA RM E55B28, 1955.
5. Standahar, Raymond M., and Geye, Richard P.: Investigation of a High-Pressure-Ratio Eight-Stage Axial-Flow Research Compressor with Two Transonic Inlet Stages. V - Preliminary Analysis of Over-All Performance of Modified Compressor. NACA RM E55A03, 1955.
6. Standahar, Raymond M., Hanson, Morgan P., and Geye, Richard P.: Investigation of a High-Pressure-Ratio Eight-Stage Axial-Flow Research Compressor with Two Transonic Inlet Stages. VI - Over-All Performance, Rotating Stall, and Blade Vibration at Low and Intermediate Compressor Speeds. NACA RM E55I13, 1955.

- 4642
CU-2 back
7. Geye, Richard P., and Lucas, James G.: Investigation of Effects of Reynolds Number on Over-All Performance of an Eight-Stage Axial-Flow Research Compressor with Two Transonic Inlet Stages. NACA RM E56L11a, 1957.
 8. NACA Subcommittee on Compressors: Standard Procedures for Rating and Testing Multistage Axial-Flow Compressors. NACA TN 1138, 1946.
 9. Burggraf, Odus R.: A Theory of Stall Propagation in Axial Compressors on the Basis of Airfoil Characteristics. Ph.D. Thesis, C.I.T., 1955.
 10. Fabri, Jean, and Siesstrunck, Raymond: Rotating Stall in Axial Flow Compressors. Preprint No. 692, Inst. Aero. Sci., 1957.
 11. Kussoy, Marvin I., and Bachkin, Daniel: Comparison of Performance of Two Aerodynamically Similar 14-Inch-Diameter Single-Stage Compressor Rotors of Different Chord Length. NACA RM E57I03, 1957.
 12. Dugan, James F., Jr.: Compressor and Turbine Matching. Ch. XVII of Aerodynamic Design of Axial-Flow Compressors, vol. III. NACA RM E56B03b, 1956.
 13. Esgar, Jack B., and Ziemer, Robert R.: Methods for Rapid Graphical Evaluation of Cooled or Uncooled Turbojet and Turpoprop Engine or Component Performance (Effects of Variable Specific Heat Included). NACA TN 3335, 1955.

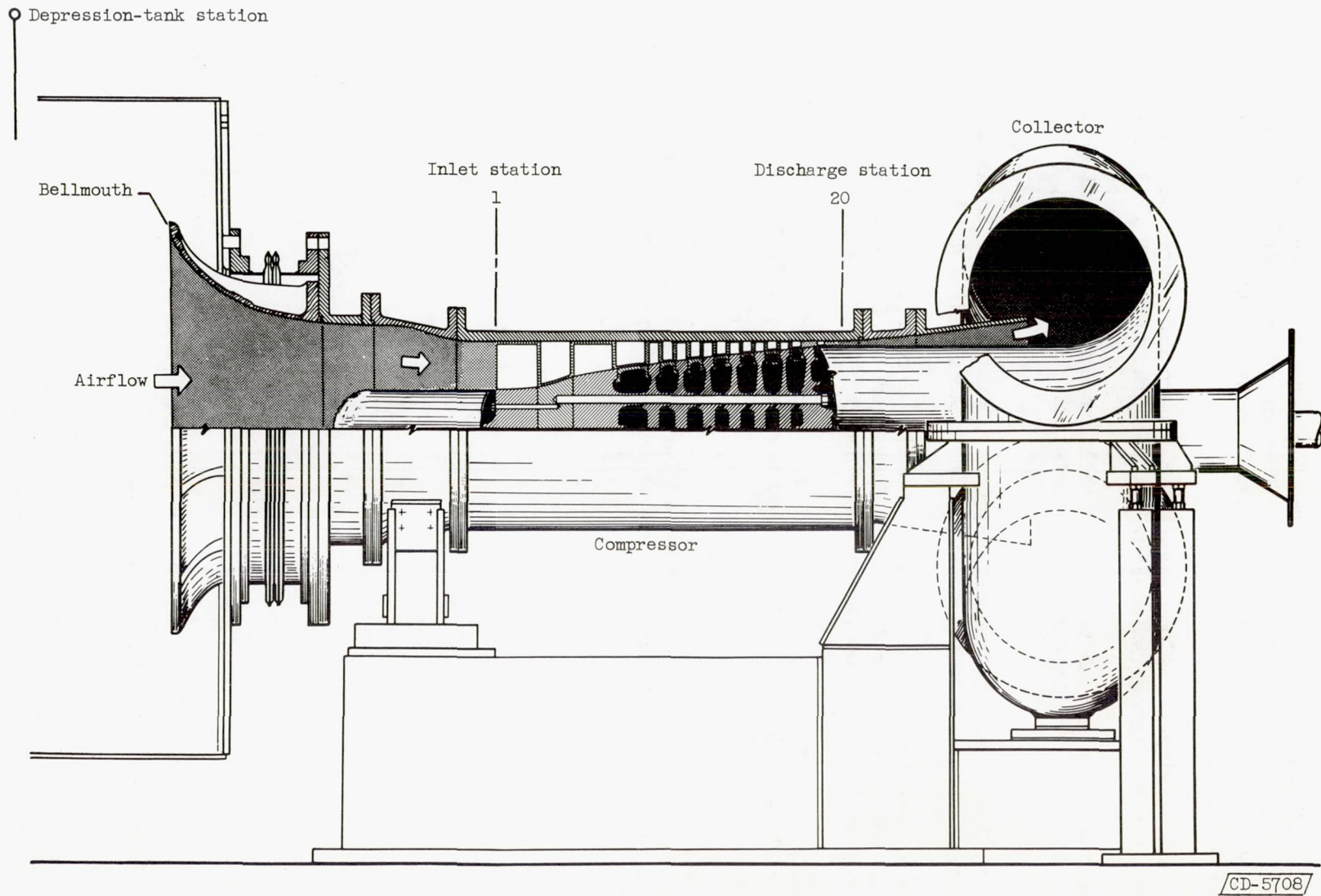
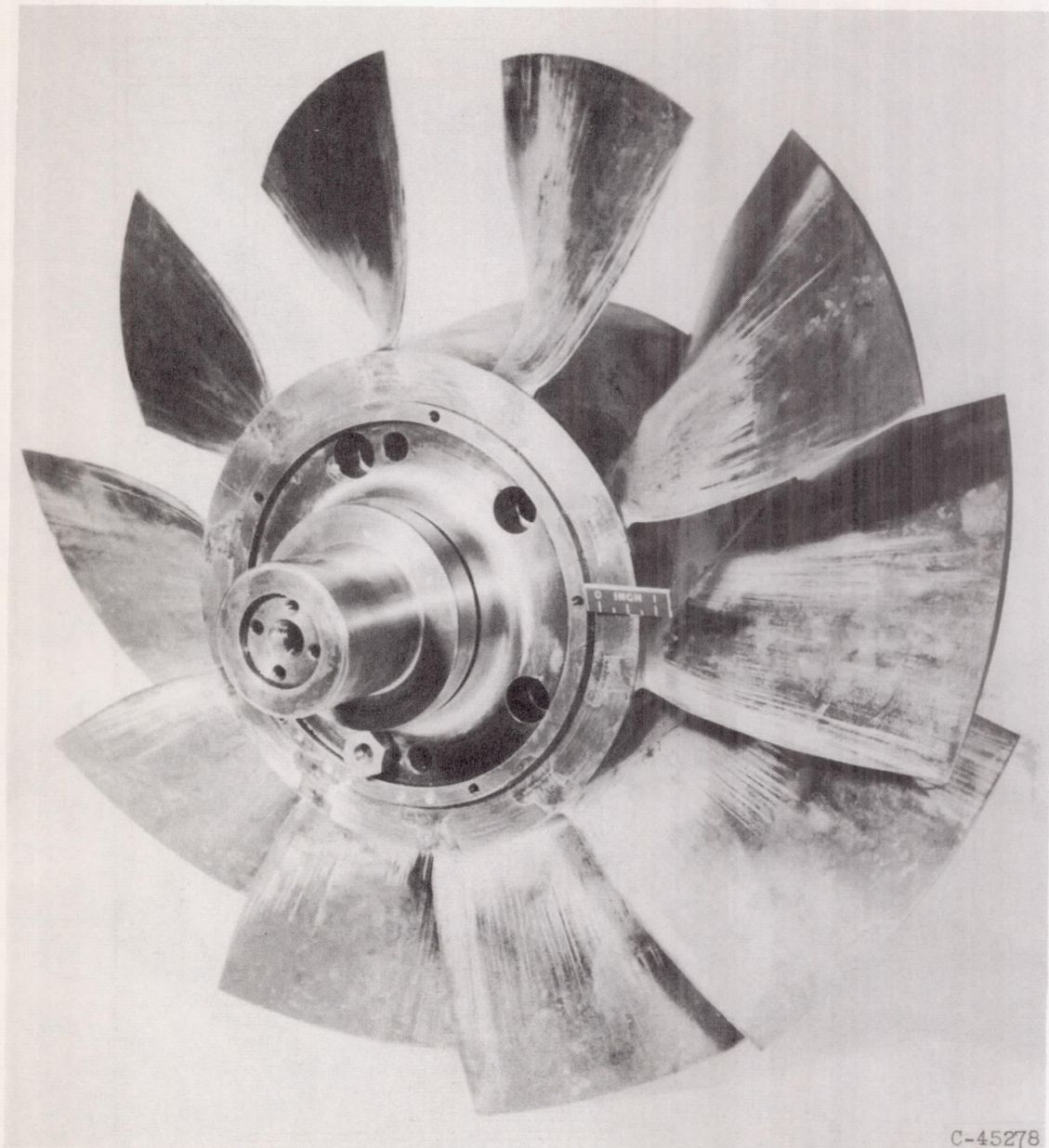


Figure 1. - Cross section of long-chord eight-stage axial-flow compressor, inlet bellmouth, and discharge collector.

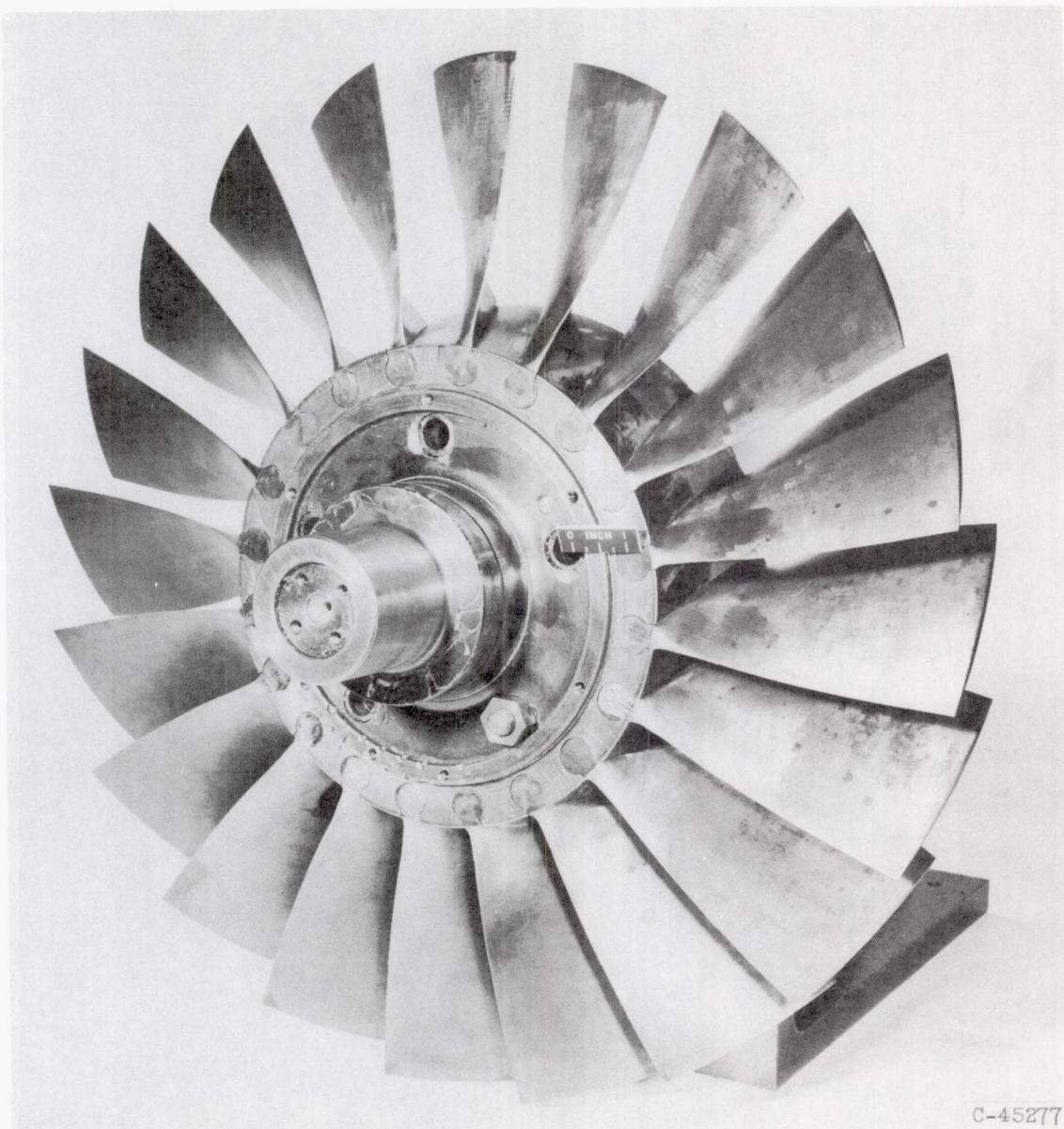
4642



C-45278

(a) First-stage rotor of long-chord compressor.

Figure 2. - First-stage rotors of long- and medium-chord compressors.



C-45277

(b) First-stage rotor of medium-chord compressor of reference 6.

Figure 2. - Concluded. First-stage rotors of long- and medium-chord compressors.

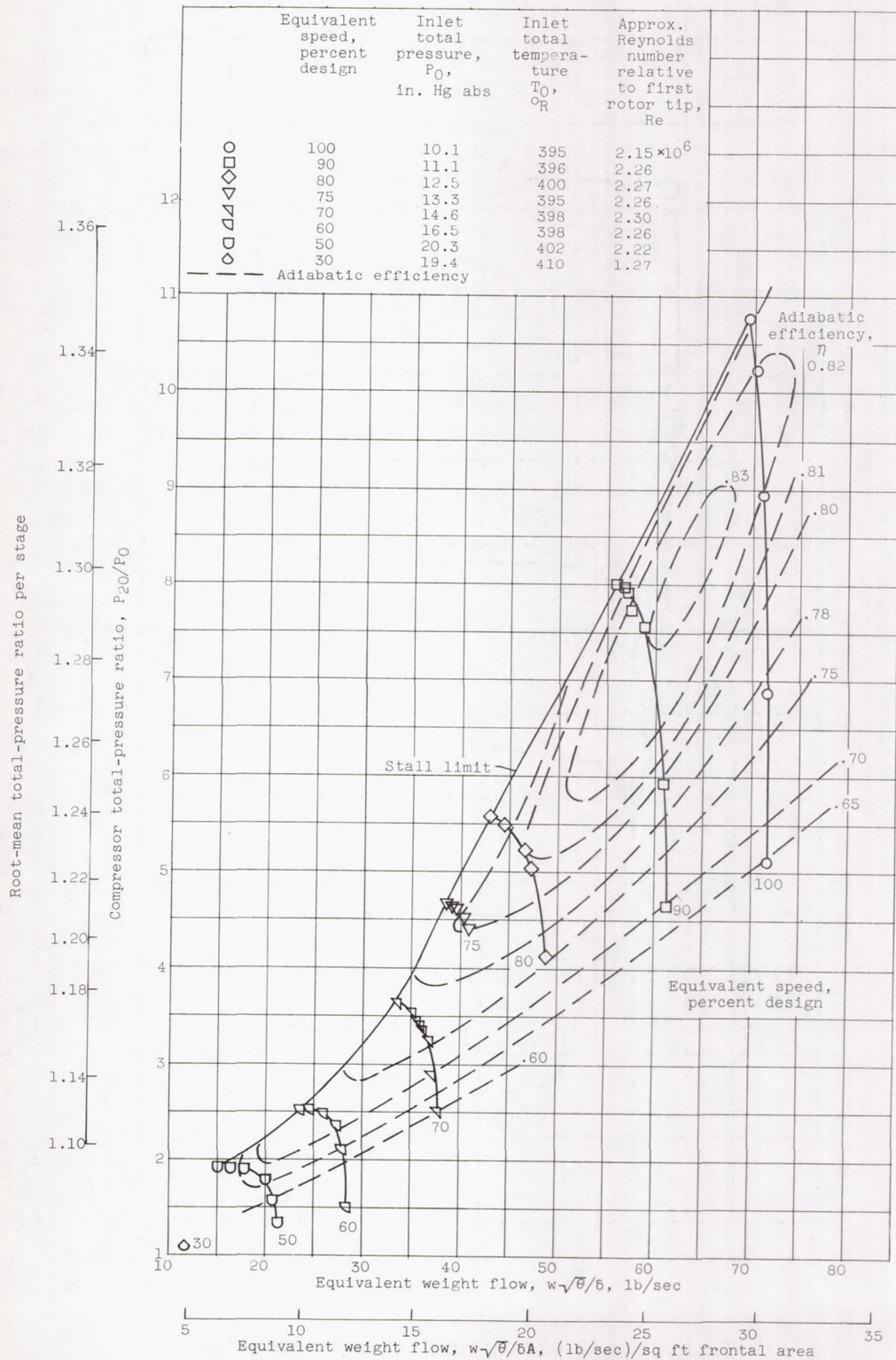


Figure 3. - Over-all performance characteristics of eight-stage axial-flow compressor with two long-chord transonic inlet stages.

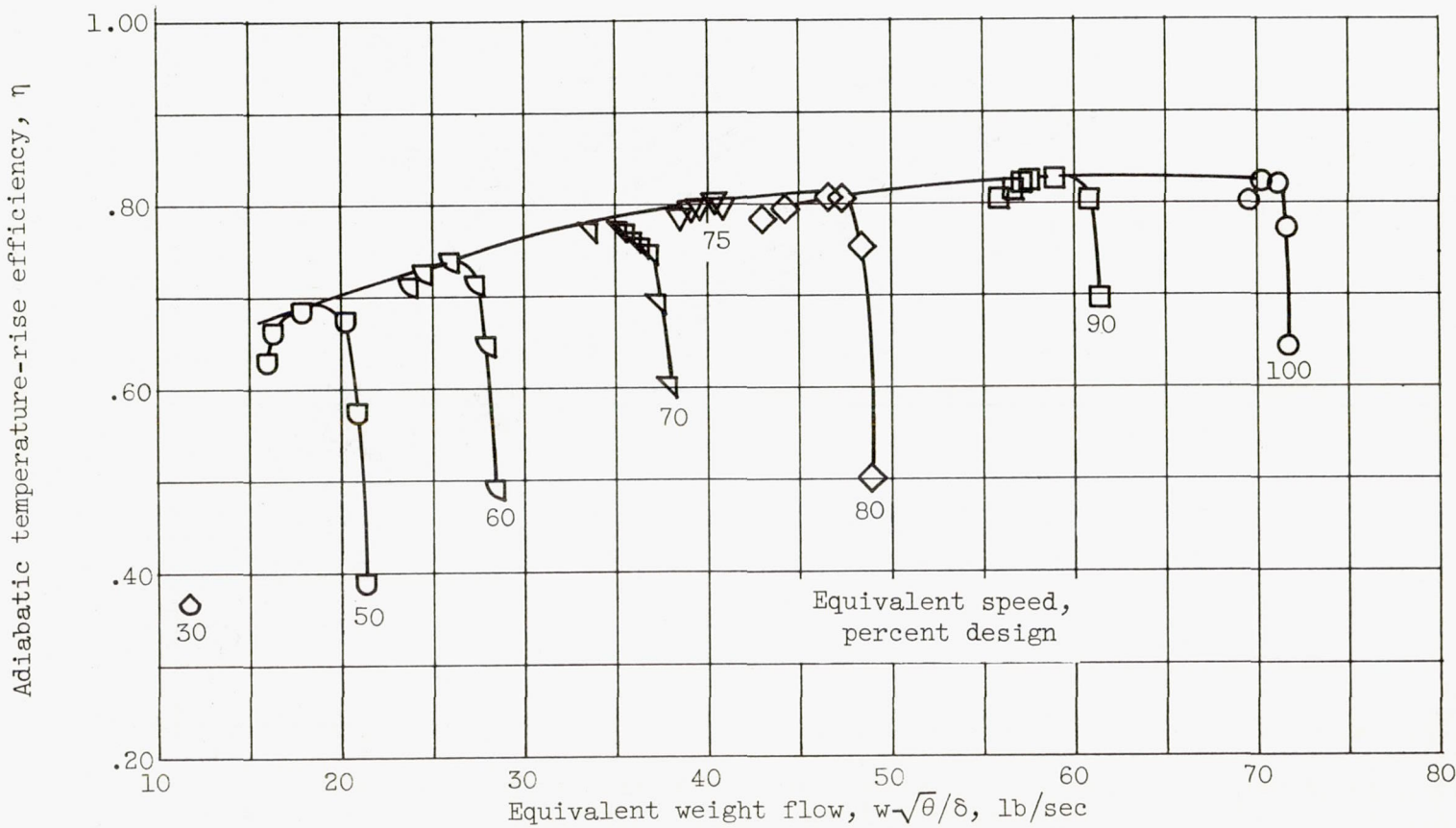


Figure 4. - Variation of adiabatic temperature-rise efficiency with speed and weight flow for long-chord compressor.

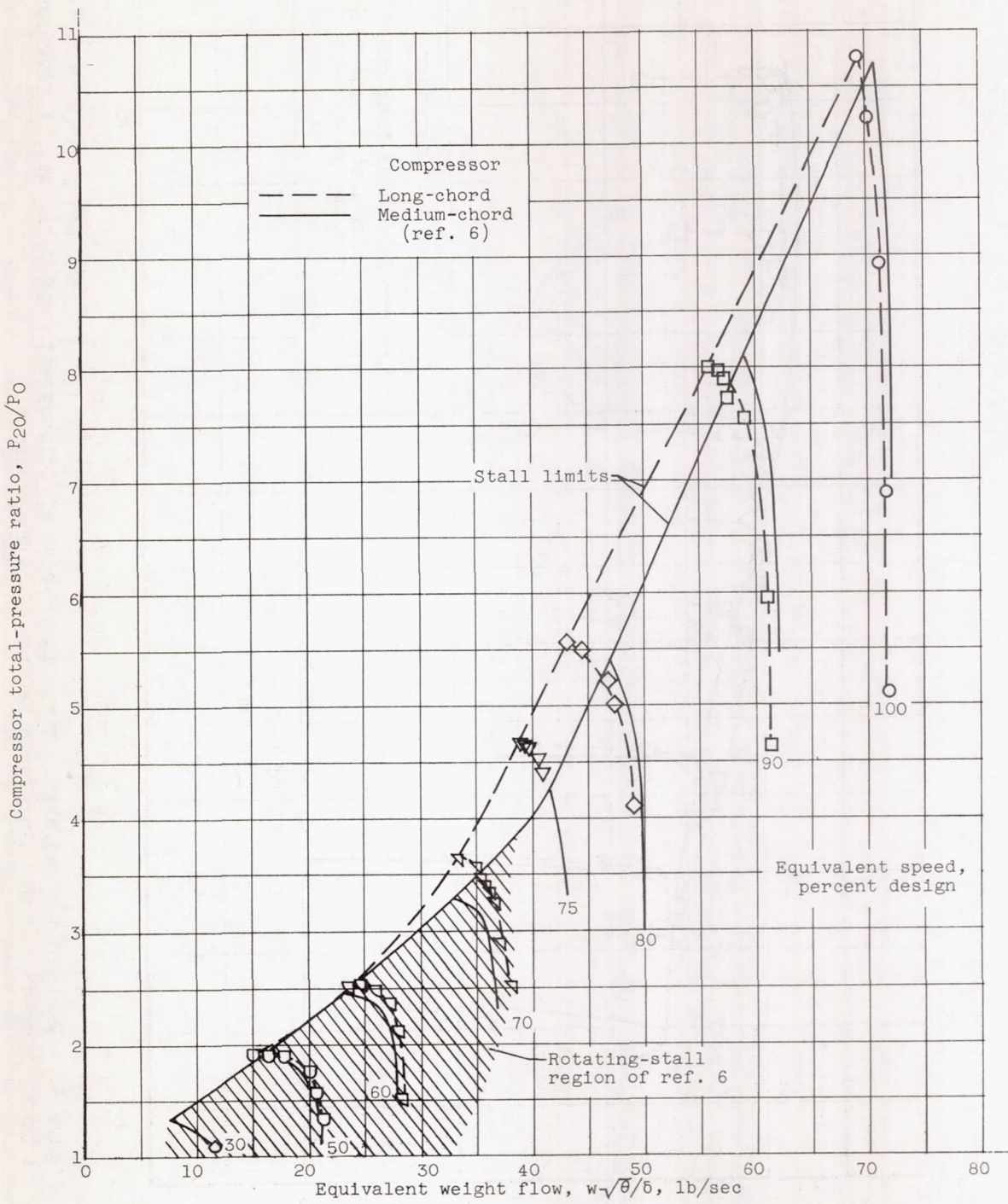


Figure 5. - Comparison of over-all performance characteristics of long- and medium-chord compressors.

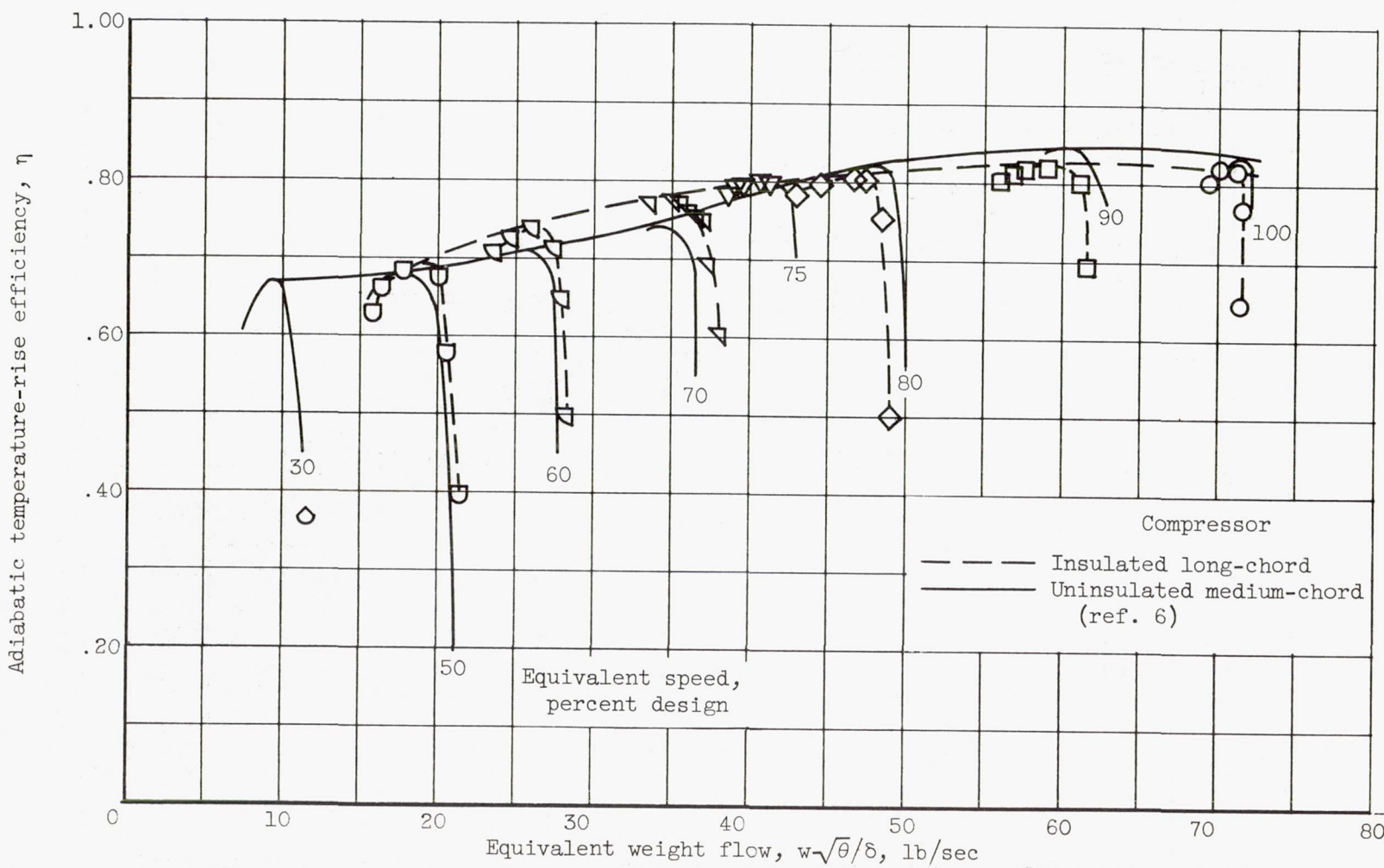


Figure 6. - Variation of adiabatic temperature-rise efficiency with speed and weight flow for insulated long-chord and uninsulated medium-chord compressors.

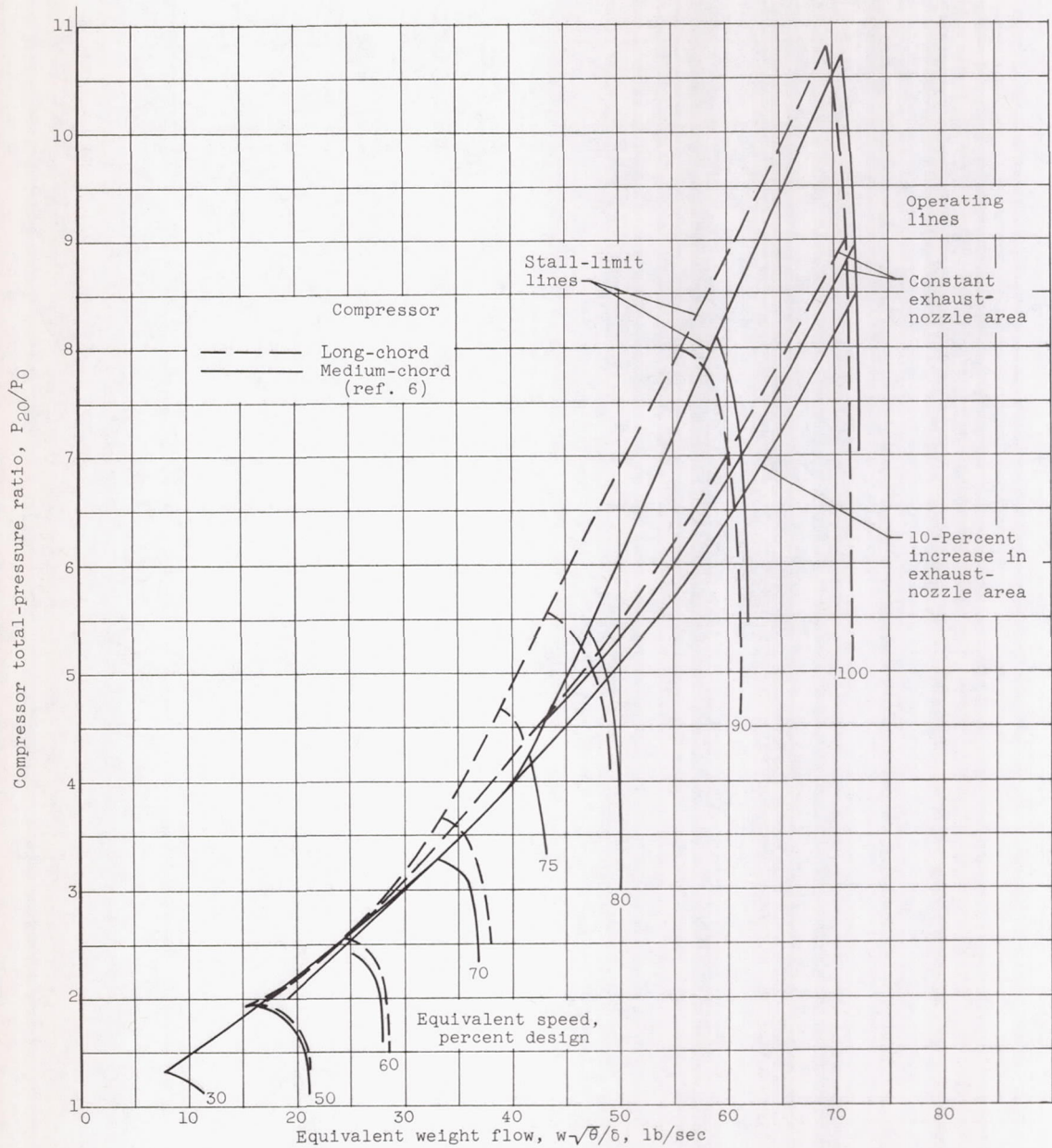


Figure 7. - Over-all performance map of long- and medium-chord compressors showing typical equilibrium operating lines.